Extreme Mechanics Letters 7 (2016) 10–17

Contents lists available at ScienceDirect

Extreme Mechanics Letters

journal homepage: www.elsevier.com/locate/eml

An algorithmic approach to multi-layer wrinkling

Emma Lejeune, Ali Javili, Christian Linder *

Department of Civil and Environmental Engineering, Stanford University, Stanford, CA 94305, USA

ARTICLE INFO

Article history:
Received 10 December 2015
Received in revised form 6 February 2016
Accepted 7 February 2016
Available online 10 February 2016

Keywords:
Wrinkling
Epidermal electronics
Geometric instability

ABSTRACT

Wrinkling, when a thin stiff film adhered to a compliant substrate deforms sinusoidally out of plane due to compression, is a well understood phenomenon in bi-layer systems. However, when there are more than two layers, the wrinkling behavior of the multi-layer system is, at present, not fully understood. In this paper, we provide an analytical solution for wrinkling in tri-layer systems where the additional layers can contribute to either the film stiffness or substrate stiffness. Then, we provide an algorithmic approach for extending our tri-layer analytical solution to systems with multiple additional layers. Our analytical solution and algorithmic approach are verified numerically using the finite element method. Using our methodology, wrinking can be predicted and controlled in multi-layer systems, with applications ranging from stretchable electronics to biomimetic design. In this paper, we demonstrate that our model can be used to understand wrinkling behavior in epidermal electronics.

1. Introduction

Though wrinkling in bi-layer systems is a well understood phenomenon [1–7], the study of wrinkling in multi-layer systems is incomplete. Multi-layer systems, as illustrated in Fig. 1, do not necessarily have a single layer clearly defined as the film or a single layer clearly defined as the substrate. Instead, there are multiple layers some of which may contribute to the axial and bending stiffness of the film and some of which may contribute to the stiffness of the substrate [8–10]. Understanding wrinkling in multi-layer systems is important for interpreting the wrinkling behavior of some biological systems, such as the gut [11–13], the skin [14–16], or the lungs [17,18]. The patterns which emerge from these biological multi-layer systems can inspire engineering design, such as engineering surfaces which utilize wrinkling to access multiple length scales and increase surface area [19–21]. In buckling based metrology, a better understanding of wrinkling in multi-layer films will enhance the study of novel multi-layer systems [22–25]. In addition, in engineering stretchable electronics, a deeper understanding of multi-layer wrinkling can be used to design systems in which wrinkling is used to prevent high levels of strain in stiff or brittle layers [26,27]. In this paper, we use epidermal electronics [28–32] as an example to motivate the study of multi-layer wrinkling. Epidermal electronics are a strong motivation because, as seen in Fig. 2, they connect to multi-layer wrinkling in two ways. First the electronic devices themselves are often multi-layer systems [28,33]. Second, the skin is a multi-layer structure thought to have as many as six mechanically distinct layers which influence its wrinkling behavior [34,35]. We present a multi-layer model suitable for capturing the wrinkling behavior of the device–skin system.

With regard to previous research specific to multi-layer wrinkling [8], we primarily build on four previous works to construct our approach to multi-layer wrinkling. First, Stafford et al. [37] proposed a method for combining thin, experimentally observed, surface layers of finite thickness with the film layer by treating the film as a composite beam. Second, Jia et al. [9] provided an

* Corresponding author.
E-mail address: linder@stanford.edu (C. Linder).

http://dx.doi.org/10.1016/j.eml.2016.02.008
2352-4316/

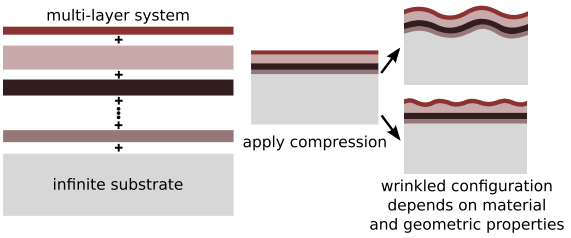

Fig. 1. When thin stiff films adhered to compliant substrates experience in plane compression, the wrinkling instability can occur. Though wrinkling in systems that consist of a single film on a substrate is well understood, wrinkling in systems with multiple layers has still not been sufficiently studied. In this paper we provide a general methodology for studying wrinkling in multi-layer systems.

analytical solution verified by numerical results to account for an intermediate layer that will combine with either the film or the substrate depending on the geometric and material properties of the system. Third, Huang et al. [38] demonstrated that after a finite substrate depth is reached, substrate depth no longer influences wrinkling behavior. Finally, in our recent work [10] we proposed an analytical solution verified by numerical results to account for wrinkling in multi-layer systems where the additional interfacial layers are assumed to be thinner than the film.

Here, we extend the solution presented in Lejeune et al. [10], which is restricted to bi-layer systems with additional *thin* interfacial layers, to systems with multiple layers that are not restricted in thickness or material properties. Then, we apply our extended multi-layer wrinkling model to a device–skin system. The rest of the paper is organized as follows. In Section 2, we clearly explain the methodology for performing this extension with an analytical solution verified by numerical results. In Section 3, we show an example of our multi-layer wrinkling model applied to epidermal electronics. Finally, we conclude our paper in Section 4.

2. Multi-layer model

The equations for critical strain ε_{cr}, critical wavelength λ_{cr}, and critical wave number n_{cr} that are sufficient to describe wrinkling initiation in a bi-layer system are quite simple. Our intention is to preserve this simplicity by extending the bi-layer solution to multiple layers following an intuitive procedure. We begin with the equation relating axial strain ε to wave number n used to derive n_{cr} for bi-layer wrinkling [1,39],

$$E_f \frac{t_f^3}{12} n^4 - E_f t_f \varepsilon n^2 = -\frac{2E_s}{\zeta} n \tag{1}$$

where E_f and E_s refer to the plane strain moduli of the film and substrate respectively, ν_s is the Poisson ratio of the substrate, t_f is film thickness, and $\zeta = (3-4\nu_s)/(1-\nu_s)^2$. In the typical applications related to the wrinkling instability, corresponding to nearly incompressible material behavior, $\nu_s \simeq 0.5$, therefore we will proceed with $\zeta = 4$. The term on the right of the equation can be understood as the influence of the infinite substrate on the film. We define t_t as the "test" depth used to determine how many layers below the film will contribute to film stiffness given the behavior of the system at instability initiation. If we think of the substrate contribution as a set of springs in parallel, with spring stiffness $K = E_s/t_t$, t_t is understood as the depth of substrate felt by the film. Given (1), the value of n_{cr} can be computed explicitly by solving $d\varepsilon/dn = 0$ with respect to n. By equating the right hand side of (1) with K, the explicit solution for t_t in a bi-layer system is computed as

$$n_{cr} = \frac{1}{t_f}\sqrt[3]{\frac{3E_s}{E_f}} \quad \text{and} \quad t_t = \frac{2}{n_{cr}}. \tag{2}$$

This is consistent with the notion that after a certain substrate depth is reached, the system will behave identically to a system with an infinite substrate [38,40]. Based on (2), it is clear that a higher E_f/E_s ratio corresponds to larger values of t_t.

In the context of wrinkling initiation in multi-layer systems, computing t_t is necessary because it will be used to determine which combination of layers contribute to either film or substrate stiffness. We define the terms "FCL" to denote film contributing layers and "SCL" to denote substrate contributing layers. For example, in a tri-layer system where the film on top is stiffer than both lower layers, computing t_t with respect to the film and intermediate layer tests if a possible buckling mode is bi-layer wrinkling entirely independent of the lowest layer. When t_t is greater than the thickness of the intermediate layer, the bi-layer equations are no longer sufficient to predict wrinkling. Therefore, a solution for wrinkling in a tri-layer system is required. To address this, we demonstrate that the equations presented in Lejeune

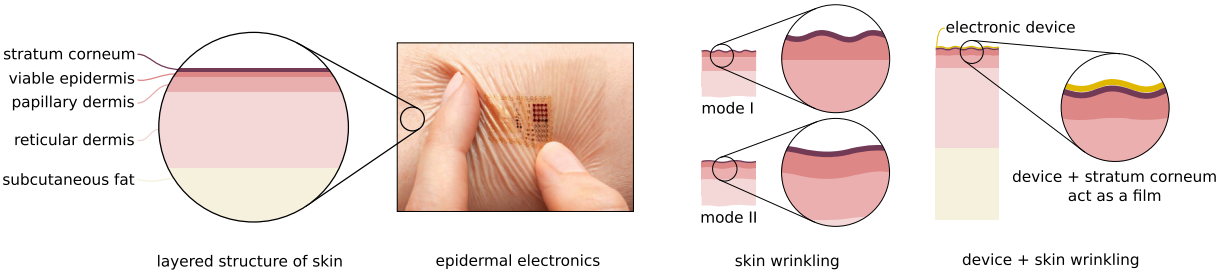

Fig. 2. This figure illustrates the connection between multi-layer wrinkling and epidermal electronics (left center experimental image published in [36]). By modeling the skin with five mechanically distinct layers [35], it is possible to obtain a better understanding of its wrinkling behavior. We find that in the device–skin system the device and stratum corneum will act as a film while the four lower layers of the skin will act as the substrate. A more detailed analysis is provided in Section 3.

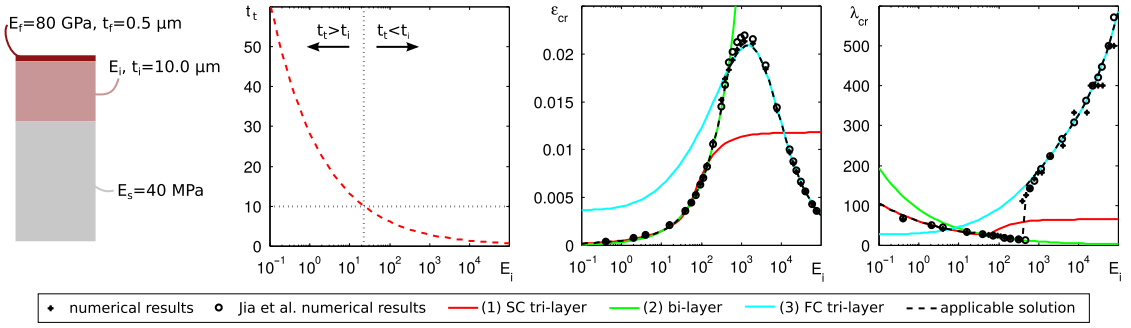

Fig. 3. Left: schematic illustration of the system evaluated. Center left: plot of t_t computed using (2) E_f, t_f and E_i, the properties of the top two layers, to highlight the point when $t_t < t_i$ and the bi-layer model is applicable rather than the substrate contributing tri-layer model. Center right: plot of ε_{cr} vs. E_i. Right: plot of λ_{cr} vs. E_i. The analytical solutions show (1) the substrate contributing tri-layer model, (2) the bi-layer model using the two upper layers, (3) the film contributing tri-layer model, and finally the applicable final solution that is a piecewise combination of these three models. The Jia et al. numerical results are conducted using the finite element method implemented in ABAQUS via a linear perturbation analysis. Our numerical results are computed using an in-house finite element code and the procedure detailed in [41]. In all plots, modulus E_i is reported in units of MPa while t_t and λ_{cr} are reported in μm. Overall, the plots shown in this figure confirm that our proposed methodology is capable of handling tri-layer systems with thick intermediate layers. We report both our numerical results and the ones present in Jia et al. [9] to emphasize that the numerical results presented in this paper are sound and reproducible and to confirm the abrupt change in wavelength reported in Jia et al.

et al. [10] for a tri-layer model with thin interfacial layers are extensible to systems with thick interfacial layers. With an intermediate layer that acts as a SCL, (1) becomes

$$E_f \frac{t_f^3}{12} n^4 - E_f t_f \varepsilon n^2 = -\frac{E_s n}{n t_i (E_s/E_i - 1) + 2} \tag{3}$$

where E_i is the plane strain intermediate layer modulus, t_i is the intermediate layer thickness [10]. The implicit equation, $\mathrm{d}\varepsilon/\mathrm{d}n = 0$ can be solved for n_{cr} and subsequently $\varepsilon_{cr} = \varepsilon(n_{cr})$. For an intermediate layer which contributes to the film stiffness (FCL), the overarching equation is identical to (1), except the bending and axial stiffness of the film must be updated to treat the multi-layer film as a composite plate. Eq. (1) becomes

$$(E_i I_i + E_f I_f) n^4 - (t_i E_i + t_f E_f) \varepsilon n^2 = -\frac{E_s n}{2} \tag{4}$$

where I_i and I_f correspond to the moment of inertia divided by width of the intermediate layer and film respectively, computed via the parallel axis theorem. The idea of combining the intermediate layer and film as composite plates was originally proposed in Stafford et al. [37] in the context of buckling based metrology, and the result is a set of explicit equations for n_{cr}, λ_{cr} and ε_{cr}.

Given these two options, FCL and SCL, the option which occurs at a lower level of strain will correspond to instability initiation [9]. In Fig. 3, ε_{cr} and λ_{cr} for a system with fixed film and substrate properties and varied intermediate layer properties are plotted. It is clearly illustrated that using the bi-layer solution where the top two layers compose the bi-layer, the SCL tri-layer solution, and the FCL tri-layer solution, instability initiation can be captured throughout the domain. The piecewise applicable solution illustrated in Fig. 3 is computed as follows. When $E_i < E_s$, t_t is used to choose between the bi-layer model and the SCL model. When $E_i > E_s$ the applicable model will be the SCL model or the FCL model, determined by computing ε_{cr} for both models and choosing the one which corresponds to a lower value of ε_{cr}. Based on Fig. 3, it is clear that our extension from a thin intermediate layer to a thick intermediate layer is validated by the good agreement with numerical results.

Like the equations proposed in Jia et al. [9], we are able to capture the entire domain of numerical results. However, for the SCL solution, the equations we use to compute ε_{cr} and λ_{cr} are different and somewhat simpler to intuitively understand and implement. Though simpler certainly does not translate to "better", our approach has the benefit of being naturally extensible to systems with more than three layers. With regard to combining multiple intermediate layers to contribute to the substrate, this extension can be conducted by treating the layers as a set of springs in series

$$t_i^{\mathrm{tot}} = t_k + t_{k+1} \quad \text{and} \quad E_i^{\mathrm{tot}} = \frac{E_k E_{k+1}(t_i + t_{i+1})}{E_i t_{i+1} + E_{k+1} t_k} \tag{5}$$

where layers k and $k+1$ are combined to a total layer stiffness, and t^{tot} and E^{tot} describe a single layer equivalent to the two layers combined. In order to compute t_t when there are intermediate layers contributing to the substrate, we use the value K, which represents the substrate contribution given in the right hand side of (3). The value of K is known after implicitly solving $\mathrm{d}\varepsilon/\mathrm{d}n = 0$. Treating the intermediate layer and substrate as springs in series means that t_t can be computed as

$$K = \frac{E_s n_{cr}}{n_{cr} t_i (E_s/E_i - 1) + 2}$$

$$t_t = \frac{E_i E_s - K E_s t_i}{K E_i}. \tag{6}$$

To combine multiple layers contributing to film stiffness, the layers are treated as a composite plate [37]. The resulting axial and bending stiffness from combining two layers can be computed as

$$\bar{y} = \frac{E_k t_k (t_{k+1} + t_k/2) + E_{k+1} t_{k+1} (t_{k+1}/2)}{E_k t_k + E_{k+1} t_{k+1}}$$

$$I_k = \frac{1}{12}t_k^3 + t_k(\bar{y} - (t_{k+1} + t_k/2))^2$$

$$I_{k+1} = \frac{1}{12}t_{k+1}^3 + t_{k+1}(\bar{y} - t_{k+1}/2)^2$$

$$[EA]_{\text{tot}} = E_k t_k + E_{k+1}t_{k+1}$$

$$[EI]_{\text{tot}} = E_k I_k + E_{k+1}I_{k+1}. \tag{7}$$

As with adding subsequent intermediate layers to the substrate, adding additional layers to the film can be conducted iteratively. If $[EA]_k^{\text{tot}}$, $[EI]_k^{\text{tot}}$ and $\bar{y}_k^{\text{tot}}$ corresponding to layer k are known, $[EA]_{k+1}$, $[EI]_{k+1}$ and $\bar{y}_{k+1}$ can be computed readily, then the total values of $[EA]_{k+1}^{\text{tot}}$, $[EI]_{k+1}^{\text{tot}}$ and $\bar{y}_{k+1}^{\text{tot}}$ corresponding to total system $k+1$ are computed as

$$\bar{y} = \frac{[EA]_k^{\text{tot}}(\bar{y}_k^{\text{tot}} + t_{k+1}) + [EA]_{k+1}t_{k+1}/2}{[EA]_k^{\text{tot}} + [EA]_{k+1}}$$

$$[EA]_{k+1}^{\text{tot}} = [EA]_k^{\text{tot}} + [EA]_{k+1}$$

$$[EI]_{k+1}^{\text{tot}} = [EI]_k^{\text{tot}} + [EA]_{k+1}^{\text{tot}}(\bar{y} - \bar{y}_k^{\text{tot}} - t_{k+1})^2 + [EI]_{k+1} + [EA]_{k+1}(\bar{y} - t_{k+1}/2)^2. \tag{8}$$

By combining (3) and (4), we obtain an expression for a system with a multi-layer film, multi-layer intermediate region and a substrate as

$$[EI]^{\text{tot}}n^4 - [EA]^{\text{tot}}\varepsilon n^2 = -\frac{E_s n}{nt_i^{\text{tot}}(E_s/E_i^{\text{tot}} - 1) + 2}. \tag{9}$$

The algorithms provided in Fig. 4 clearly illustrate the procedure for determining which layers contribute to the film and which layers contribute to the substrate such that (9) can be applied. Just as with the bi-layer solution, some systems will not be good candidates for applying the analytical solution and will require numerical analysis. This is particularly the case when the total sum of SCLs is not sufficiently thick, when the total sum of FCLs is too close to the wrinkle wavelength, when the conditions of small strain are violated or when different modes of instability may occur at nearly the same level of strain. Notable alternative methods for quantifying surface instabilities in systems with depth varying material properties include the state space method [44], and the finite element method [40], which, unlike our method, do not approximate layers as either thin plates (FCLs) or linear springs (intermediate SCLs).

Using our method, it is clear that tri-layer problems can be understood very intuitively and interpreted directly from the equations in Section 2. For systems with more than three layers, the algorithm presented in Fig. 4 proves useful for describing our implementation. To further demonstrate the validity of our approach for systems with more than three layers, we compare the algorithmic solution for a four layer system to numerical results [41]. The geometry and material properties of the system tested are shown in Fig. 5. In this system, the layers of the substrate becomes stiffer with increasing depth, so the algorithm illustrated in Fig. 4 is used to determine the analytical solution. In the results plotted in Fig. 5, the properties of the intermediate layers and substrate are held fixed while the film stiffness is increased. As E_f increases, the depth of substrate influencing film behavior increases. Therefore, when E_f is very low, the first intermediate layer acts as the substrate. When E_f, and subsequently t_s, increases, the second intermediate layer and substrate layer both contribute to instability initiation. Based on the good agreement between our numerical and analytical solutions, it is clear that our approach is valid for the system tested. In Fig. 5, the analytical solutions for the bi-layer system of the film and each subsequent layer are also shown to illustrate that while the curves are the same shape, the predicted values are sufficiently different such that it is evident that the close agreement between our analytical and numerical solution is not coincidental.

3. Application to epidermal electronics

As illustrated in Fig. 2, images and studies of the human skin indicate that it has a multi-layer structure [45]. Here, we present a model of the skin which has five mechanically distinct layers [35]. Due to the variability in parameters reported in the literature [46–50], both due to differences in experimental set up and variation across subjects and locations on the body [51], the parameters chosen for our model are approximations. Similar to the abrupt mode switch illustrated in Fig. 3, stiffening of skin during the aging process is shown to cause an abrupt switch between mode I wrinkling, where the stratum corneum acts as the film, and mode II wrinkling where the stratum corneum and viable epidermis act as a composite film. With our approach to multi-layer wrinkling, we are able to confirm that this switch is plausible. Previous predictions of this switch, while insightful, relied on very approximate analytical and numerical results [35]. Of course, more accurate quantification of geometry and parameters is required to make quantitative or prescriptive conclusions about wrinkling in the skin. However, this prediction of a mode switch with an abrupt jump in λ_{cr} has been observed experimentally in a study of wrinkling response to applied compression in facial skin for subjects of varied age [52]. Our analysis also indicates that there are multiple systems (combinations of different FCL or SCL) which can potentially wrinkle in the skin, and that an increase in ε_{cr} may induce longer wavelength wrinkling. For example, wrinkling in the stratum corneum layer may occur first, and then wrinkling of the stratum corneum and viable epidermis acting as a composite film may become superimposed at a higher level of strain. It is also possible that the deformation induced by the lower wrinkling modes will not heavily influence the timing and appearance of the higher modes because the differences in length scale may render wrinkling induced deformation negligible. This is consistent with experimental observations which indicate that multiple superimposed wavelengths may be observed in skin under high levels of compression [14,16].

The design of epidermal electronics is highly varied and rapidly evolving [28,30]. Here, we consider a simplified system in which an electronic device is treated as an additional layer on the surface of the skin. With our model, we can qualitatively understand what occurs when the device–skin system is subject to compression. Fig. 6

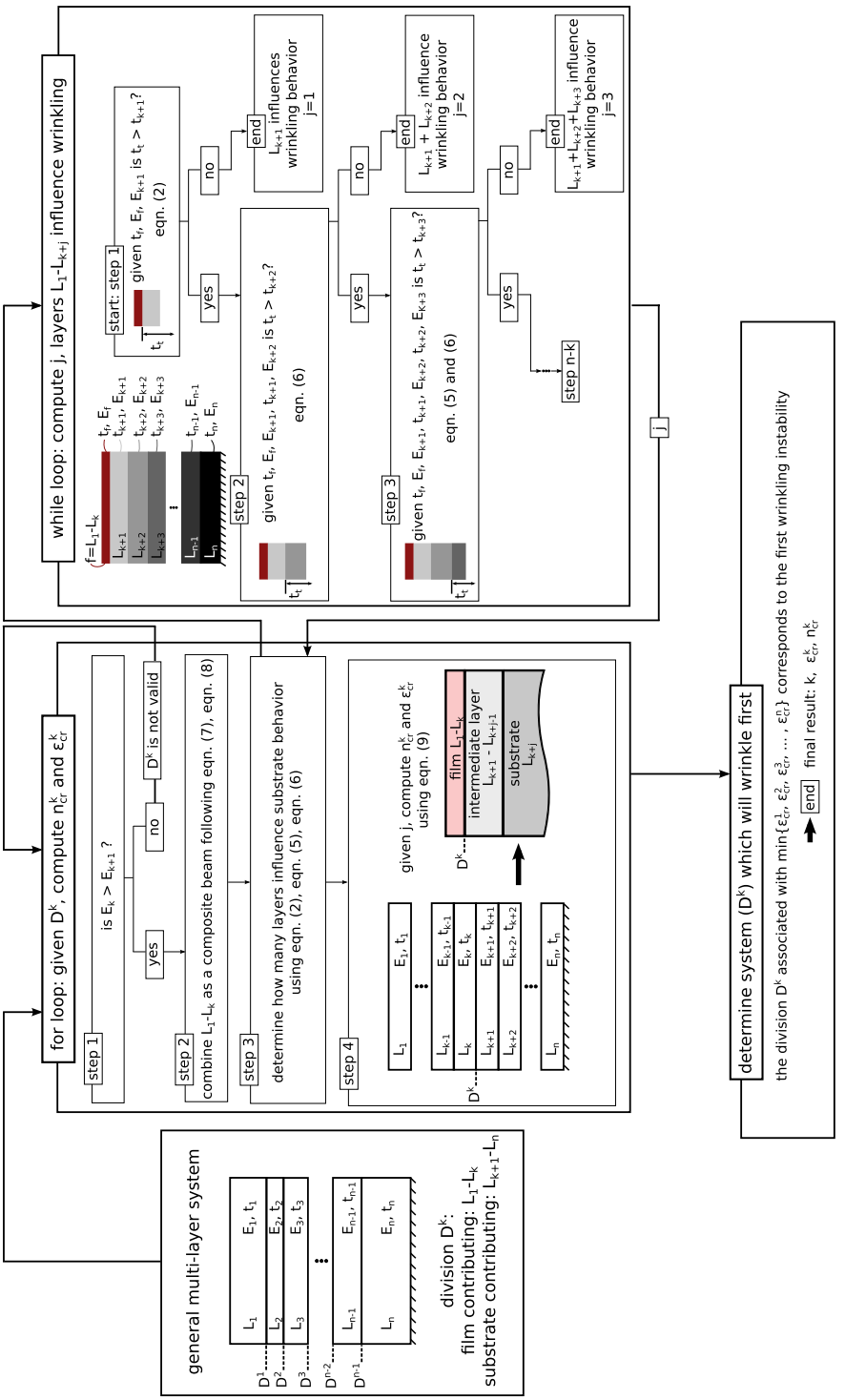

Fig. 4. Given the equations presented in Section 2, this algorithm summarizes their implementation. It is important to note that some systems will not exhibit wrinkling at all, and, that this algorithm does not check for forms of geometric instability other than wrinkling such as creases [42,43]. If the final computed value of ε_{cr} exceeds 0.456, then there is reason for caution because 0.456 corresponds to the upper limit of the bi-layer solution for a film and substrate with identical stiffness [39]. And, as with bi-layer wrinkling, some systems require numerical analysis because they deviate significantly from the analytical solution assumptions.

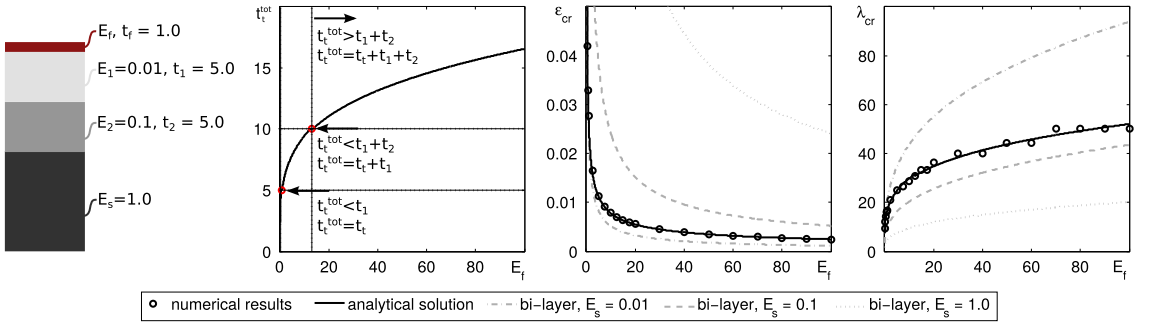

Fig. 5. Left: schematic diagram of the system tested analytically and numerically. Left Center: depth below film engaged with respect to different values of E_f with a marked transition and additional layers become engaged. Right Center: n_{cr} plotted with respect to E_f for both numerical and analytical results, the incorrect bi-layer solutions are plotted for comparison. Right: ε_{cr} plotted with respect to E_f for both numerical and analytical results, the incorrect bi-layer solutions are plotted for comparison. The units of E are reported are MPa and t_t and λ_{cr} are reported in μm.

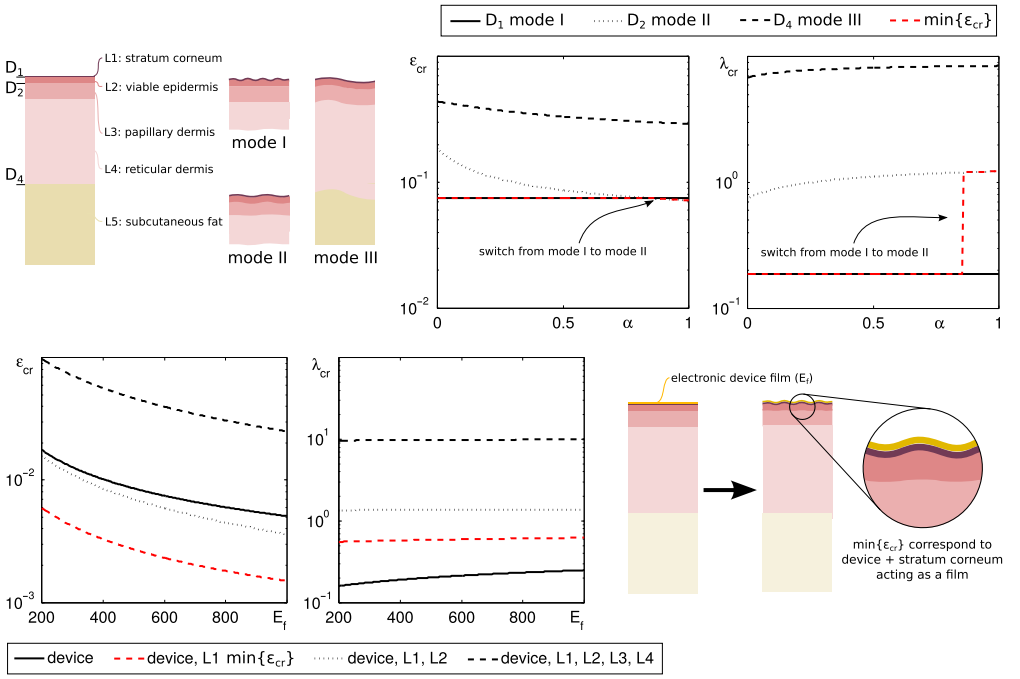

Fig. 6. Upper row: wrinkling in a five layer model of human skin. Lower row: wrinkling in a model of human skin with a device adhered to the top. In the upper row, α represents the degree to which the skin has aged where the modulus of each layer varies linearly between "young" and "old" values according to α [35]. Because there is much variability in the literature for mechanical properties of skin [45], the values taken here are order of magnitude approximations. The un-aged moduli ($\alpha = 0$), from top to bottom are 1 MPa, 0.1 MPa, 0.05 MPa, 0.1 MPa and 0.075 MPa. The aged moduli are 10 MPa, 1 MPa, 0.1 MPa, 0.2 MPa, 0.15 MPa. Changes in skin thickness due to aging were neglected, from top to bottom the thickness of each layer is 0.02 mm, 0.08 mm, 0.2 mm, 1 mm and 2 mm similar to parameters chosen in [35]. In the lower row, skin properties corresponding to $\alpha = 0.5$ were chosen while the stiffness of the device E_f was varied in units of MPa. The device layer is 0.005 mm thick. Besides the highly intuitive result, that increasing E_f results in lower ε_{cr} and higher λ_{cr}, it is noteworthy that the predicted mode of wrinkling, corresponding to minimum ε_{cr} is the device and stratum corneum acting as a composite film while the remainder of the skin acts as a substrate.

compares ε_{cr} and λ_{cr} of the device–skin system with different device stiffness to the behavior of the skin alone. The predicted decrease in ε_{cr} and increase in λ_{cr} is a highly intuitive result given that the additional layer increases the stiffness of any film or composite film layer that may arise. However, our model also predicts that the first mode of wrinkling to occur will be the system in which the device and stratum corneum act as a composite film. Before applying our model, it was unclear if the lowest value of ε_{cr} would correspond to the device acting as a film with the entire skin as a substrate or if layers of the skin would also act as a film. The results of our study are illustrated in Fig. 6. Moving forward, the notion that the device and the stratum corneum wrinkle together may contribute to the understanding of buckling delamination in these systems [30,33,53,54]. Though the results presented here are only valid for a given set of parameters, our model has the benefit of being easily implemented and tested for alternative layered device configurations or skin properties.

4. Conclusion

In this paper, we outline a procedure for computing the analytical solution for wrinkling instability initiation in multi-layer systems. We begin by presenting our previously developed solution for multi-layer wrinkling in systems with a limited number of very thin interfacial layers. Then, we extend this solution to multi-layer systems with an unlimited number of layers and unconstrained layer thickness. Performing this extension has utility in many areas, ranging from stretchable electronics [26,55], to understanding biological pattern formation [56], to manufacturing biomimetic surface topology [20]. In this paper, we demonstrate the utility of our model for predicting multi-layer wrinkling in epidermal electronics. The configuration of these systems in highly varied and rapidly evolving which further motives our presentation of a general model for multi-layer wrinkling.

Acknowledgment

Financial support for this research was provided by the National Science Foundation through CAREER Award CMMI-1553638 and the National Science Foundation Graduate Research Fellowship under Grant No. DGE-114747.

References

[1] H.G. Allen, Analysis and Design of Structural Sandwich Panels: The Commonwealth and International Library: Structures and Solid Body Mechanics Division, Elsevier, 2013.
[2] Z. Huang, W. Hong, Z. Suo, Evolution of wrinkles in hard films on soft substrates, Phys. Rev. E 70 (2004) 030601.
[3] Y. Mei, S. Kiravittaya, S. Harazim, O.G. Schmidt, Principles and applications of micro and nanoscale wrinkles, Mater. Sci. Eng. R Rep. 70 (3–6) (2010) 209–224.
[4] H. Mei, R. Huang, J.Y. Chung, C.M. Stafford, H.H. Yu, Buckling modes of elastic thin films on elastic substrates, Appl. Phys. Lett. 90 (15) (2007) 1–4.
[5] J. Song, H. Jiang, Z.J. Liu, D.Y. Khang, Y. Huang, J.A. Rogers, C. Lu, C.G. Koh, Buckling of a stiff thin film on a compliant substrate in large deformation, Internat. J. Solids Structures 45 (10) (2008) 3107–3121.
[6] S. Wang, J. Song, D.H. Kim, Y. Huang, J.A. Rogers, Local versus global buckling of thin films on elastomeric substrates, Appl. Phys. Lett. 93 (2) (2008) 3–5.
[7] Y. Zhao, X. Han, G. Li, C. Lu, Y. Cao, X.-Q. Feng, H. Gao, Effect of lateral dimension on the surface wrinkling of a thin film on compliant substrate induced by differential growth/swelling, J. Mech. Phys. Solids 83 (2015) 129–145.
[8] H. Cheng, Y. Zhang, K.C. Hwang, J.A. Rogers, Y. Huang, Buckling of a stiff thin film on a pre-strained bi-layer substrate, Internat. J. Solids Structures 51 (18) (2014) 3113–3118.
[9] F. Jia, Y.-P. Cao, T.-S. Liu, Y. Jiang, X.-Q. Feng, S.-W. Yu, Wrinkling of a bilayer resting on a soft substrate under in-plane compression, Phil. Mag. 92 (12) (2012) 1554–1568.
[10] E. Lejeune, A. Javili, C. Linder, Understanding geometric instabilities in thin films via a multi-layer model, Soft Matter 12 (2016) 806–816.
[11] M. Ben Amar, F. Jia, Anisotropic growth shapes intestinal tissues during embryogenesis, Proc. Natl. Acad. Sci. USA 110 (26) (2013) 10525–10530.
[12] E. Hannezo, J. Prost, J.F. Joanny, Instabilities of monolayered epithelia: Shape and structure of villi and crypts, Phys. Rev. Lett. 107 (August) (2011) 1–5.
[13] A.E. Shyer, T. Tallinen, N.L. Nerurkar, Z. Wei, E.S. Gil, D.L. Kaplan, C.J. Tabin, L. Mahadevan, Villification: how the gut gets its villi, Science 342 (6155) (2013) 212–218.
[14] C. Flynn, B.A.O. Mccormack, Finite element modelling of forearm skin wrinkling, Skin Res. Technol. 14 (3) (2008) 261–269.
[15] C. Flynn, B.A.O. McCormack, A three-layer model of skin and its application in simulating wrinkling, Comput. Methods Biomech. Biomed. Eng. 12 (2) (2009) 125–134.
[16] C. Flynn, B.A.O. Mccormack, Simulating the wrinkling and ageing of skin with a multi-layer finite element model, J. Biomech. 43 (3) (2010) 442–448.
[17] S.-H. Chung, J.H. Lee, J.-H. Yoon, H.K. Lee, K.Y. Seo, Multi-layered culture of primary human conjunctival epithelial cells producing MUC5AC, Exp. Eye Res. 85 (2) (2007) 226–233.
[18] M. Eskandari, M.R. Pfaller, E. Kuhl, On the role of mechanics in chronic lung disease, Materials 6 (12) (2013) 5639–5658.
[19] H.E. Jeong, M.K. Kwak, K.Y. Suh, Stretchable, adhesion-tunable dry adhesive by surface wrinkling, Langmuir 26 (4) (2010) 2223–2226.
[20] J.H. Lee, H.W. Ro, R. Huang, P. Lemaillet, T.a. Germer, C.L. Soles, C.M. Stafford, Anisotropic, hierarchical surface patterns via surface wrinkling of nanopatterned polymer films, Nano Lett. 12 (11) (2012) 5995–5999.
[21] A. Schweikart, A. Fery, Controlled wrinkling as a novel method for the fabrication of patterned surfaces, Microchim. Acta 165 (3–4) (2009) 249–263.
[22] J.Y. Chung, A.J. Nolte, C.M. Stafford, Surface wrinkling: A versatile platform for measuring thin-film properties, Adv. Mater. 23 (3) (2011) 349–368.
[23] C. Lu, I. Dönch, M. Nolte, A. Fery, Au nanoparticle-based multilayer ultrathin films with covalently linked nanostractures: Spraying layer-by-layer assembly and mechanical property characterization, Chem. Mater. 18 (26) (2006) 6204–6210.
[24] A.J. Nolte, M.F. Rubner, R.E. Cohen, Determining the Young's Modulus of polyelectrolyte multilayer films via stress-induced mechanical buckling instabilities, Macromolecules 38 (2005) 5367–5370.
[25] A.J. Nolte, R.E. Cohen, M.F. Rubner, A two-plate buckling technique for thin film modulus measurements: Applications to poly electrolyte multilayers, Macromolecules 39 (14) (2006) 4841–4847.
[26] D.Y. Khang, J.A. Rogers, H.H. Lee, Mechanical buckling: Mechanics, metrology, and stretchable electronics, Adv. Funct. Mater. 19 (10) (2009) 1526–1536.
[27] Y. Sun, W.M. Choi, H. Jiang, Y.Y. Huang, J.A. Rogers, Controlled buckling of semiconductor nanoribbons for stretchable electronics, Nature Nanotechnology 1 (3) (2006) 201–207.
[28] K.-I. Jang, S.Y. Han, S. Xu, K.E. Mathewson, Y. Zhang, J.-W. Jeong, G.-T. Kim, R.C. Webb, J.W. Lee, T.J. Dawidczyk, R.H. Kim, Y.M. Song, W.-H. Yeo, S. Kim, H. Cheng, S.I. Rhee, J. Chung, B. Kim, H.U. Chung, D. Lee, Y. Yang, M. Cho, J.G. Gaspar, R. Carbonari, M. Fabiani, G. Gratton, Y. Huang, J.A. Rogers, Rugged and breathable forms of stretchable electronics with adherent composite substrates for transcutaneous monitoring, Nature Commun. 5 (2014) 4779.
[29] M. Kaltenbrunner, T. Sekitani, J. Reeder, T. Yokota, K. Kuribara, T. Tokuhara, M. Drack, R. Schwödiauer, I. Graz, S. Bauer-Gogonea, S. Bauer, T. Someya, An ultra-lightweight design for imperceptible plastic electronics, Nature 499 (7459) (2013) 458–463.
[30] D.-H. Kim, N. Lu, R. Ma, Y.-S. Kim, R.-H. Kim, S. Wang, J. Wu, S.M. Won, H. Tao, A. Islam, K.J. Yu, T.-i. Kim, R. Chowdhury, M. Ying, L. Xu, M. Li, H.-J. Chung, H. Keum, M. McCormick, P. Liu, Y.-W. Zhang, F.G. Omenetto, Y. Huang, T. Coleman, J.A. Rogers, Epidermal electronics, Science 333 (September) (2011) 838–844.
[31] J.J.S. Norton, D.S. Lee, J.W. Lee, W. Lee, O. Kwon, P. Won, S.-Y. Jung, H. Cheng, J.-W. Jeong, A. Akce, S. Umunna, I. Na, Y.H. Kwon, X.-Q. Wang, Z. Liu, U. Paik, Y. Huang, T. Bretl, W.-H. Yeo, J.A. Rogers, Soft, curved electrode systems capable of integration on the auricle as a persistent brain–computer interface, Proc. Natl. Acad. Sci. 112 (13) (2015) 201424875.
[32] W.H. Yeo, Y.S. Kim, J. Lee, A. Ameen, L. Shi, M. Li, S. Wang, R. Ma, S.H. Jin, Z. Kang, Y. Huang, J.A. Rogers, Multifunctional epidermal electronics printed directly onto the skin, Adv. Mater. 25 (20) (2013) 2773–2778.
[33] S. Wang, M. Li, J. Wu, D.-H. Kim, N. Lu, Y. Su, Z. Kang, Y. Huang, J.A. Rogers, Mechanics of epidermal electronics, J. Appl. Mech. 79 (3) (2012) 031022.
[34] F.M. Hendriks, D. Brokken, C.W.J. Oomens, D.L. Bader, F.P.T. Baaijens, The relative contributions of different skin layers to the mechanical behavior of human skin in vivo using suction experiments, Med. Eng. Phys. 28 (3) (2006) 259–266.
[35] O. Kuwazuru, J. Saothong, N. Yoshikawa, Evaluation of ageing effects on skin wrinkle by finite element method, J. Biomech. Sci. Eng. 3 (3) (2008) 368–379.
[36] Biostamp temporary tattoo electronic circuits by MC10, Dezeen Magazine.

[37] C.M. Stafford, B.D. Vogt, C. Harrison, D. Julthongpiput, R. Huang, Elastic moduli of ultrathin amorphous polymer films, Macromolecules 39 (15) (2006) 5095–5099.
[38] Z. Huang, W. Hong, Z. Suo, Nonlinear analyses of wrinkles in a film bonded to a compliant substrate, J. Mech. Phys. Solids 53 (9) (2005) 2101–2118.
[39] M.A. Biot, On bending of an infinite beam on an elastic Foundation, J. Appl. Math. Mech. 22 (5) (1937) 984–988.
[40] D. Lee, N. Triantafyllidis, J.R. Barber, M.D. Thouless, Surface instability of an elastic half space with material properties varying with depth, J. Mech. Phys. Solids 56 (2008) 858–868.
[41] A. Javili, B. Dortdivanlioglu, E. Kuhl, C. Linder, Computational aspects of growth-induced instabilities through eigenvalue analysis, Comput. Mech. 56 (3) (2015) 405–420.
[42] Y. Cao, J.W. Hutchinson, Wrinkling phenomena in neo-hookean film/substrate bilayers, J. Appl. Mech. 79 (May) (2012) 031019.
[43] M. Diab, T. Zhang, R. Zhao, H. Gao, K.-S. Kim, Ruga mechanics of creasing: from instantaneous to setback creases, Proc. R. Soc. Ser. A Math. Phys. Eng. Sci. 469 (2157) (2013) 20120753.
[44] Z. Wu, J. Meng, Y. Liu, H. Li, R. Huang, A state space method for surface instability of elastic layers with material properties varying in thickness direction, J. Appl. Mech. 81 (8) (2014) 81003.
[45] M.F. Leyva-Mendivil, A. Page, N.W. Bressloff, G. Limbert, A mechanistic insight into the mechanical role of the stratum corneum during stretching and compression of the skin, J. Mech. Behav. Biomed. Mater. 49 (0) (2015) 197–219.
[46] M. Geerligs, L. van Breemen, G. Peters, P. Ackermans, F. Baaijens, C. Oomens, In vitro indentation to determine the mechanical properties of epidermis, J. Biomech. 44 (6) (2011) 1176–1181.
[47] J.-L. Gennisson, T. Baldeweck, M. Tanter, S. Catheline, M. Fink, L. Sandrin, C. Cornillon, B. Querleux, Assessment of elastic parameters of human skin using dynamic elastography, IEEE Trans. Ultrason. Ferroelectr. Freq. Control 51 (8) (2004) 980–989.
[48] C. Li, G. Guan, R. Reif, Z. Huang, R.K. Wang, Determining elastic properties of skin by measuring surface waves from an impulse mechanical stimulus using phase-sensitive optical coherence tomography, J. R. Soc. Interface 9 (70) (2012) 831–841.
[49] X.L.X. Liang, S. Boppart, Biomechanical properties of in vivo human skin from dynamic optical coherence elastography, IEEE Trans. Biomed. Eng. 57 (4) (2010) 953–959.
[50] J. Welzel, E. Lankenau, R. Birngruber, R. Engelhardt, Optical coherence tomography of the human skin, J. Am. Acad. Dermatol. 37 (6) (1997) 958–963.
[51] F. Hendriks, Mechanical behaviour of human skin in vivo, Biomed. Eng. 4 (1969) 322–327.
[52] O. Kuwazuru, K. Miyamoto, N. Yoshikawa, S. Imayama, Skin wrinkling morphology changes suddenly in the early 30s, Skin Res. Technol. 18 (4) (2012) 495–503.
[53] H. Cheng, S. Wang, Mechanics of interfacial delamination in epidermal electronics systems, J. Appl. Mech. 81 (4) (2013) 044501.
[54] H. Mei, R. Huang, Wrinkling and delamination of thin films on compliant substrates 2. Wrinkling analysis, in: 13th International Conference on Fracture, 2013, pp. 1–9.
[55] D.-Y. Khang, H. Jiang, Y. Huang, J.A. Rogers, A stretchable form of single-crystal, Science 311 (January) (2006) 208–212.
[56] P. Ciarletta, V. Balbi, E. Kuhl, Pattern selection in growing tubular tissues, Phys. Rev. Lett. 113 (24) (2014) 248101.